International Journal of Multimedia and Ubiquitous Engineering
Vol.11, No.6 (2016), pp.27-34
http://dx.doi.org/10.14257/ijmue.2016.11.6.03

Infrared Camera Calibration in the 3D Temperature Field Reconstruction

Sun Xiaoming, Wu Haibin, Wang Wei, Liubo and Cui Guoguang

The higher Educational Key Laboratory for Measuring & Control Technology and Instrumentations
Harbin University of Science and Technology
Heilongjiang Province, Harbin 150080, China
xiaoming_66881982@163.com

Abstract

In order to reconstruct the 3D temperature field based on the binocular vision system, we carry out a research on the calibration of the infrared camera. To start with, we make a calibration board which can be clearly identified by the infrared camera; then, with the help of OpenCV, we implement the calibration of two infrared cameras respectively and rectify the infrared images. According to the parameters obtained from the single infrared camera calibration, we accomplish the stereo calibration. The experimental results show that the average reprojecting error is below 0.14 pixels and when using the system to carry out a real measurement, the average error is 3.12%. The feasibility of the proposed calibration approach is verified, the experimental measurement results is close to the ground truth.

Keywords: *3D temperature field; Vision measurement; Infrared camera calibration; Infrared image matchup*

1. Introduction

With the development of computer technology, 3D reconstruction has been widely applied. And consequently, 3D temperature field reconstruction based on infrared images has also shown its advantages in various fields. When reconstruct the 3D temperature field, the calibration of the infrared camera is the original step and one of the most important steps.

Currently, approaches for the visible light camera calibration are a lot and the calibration result is pretty accurate. The earliest stereo-camera calibration method was proposed by D. Gennery (1979). Then, scholars began to study calibration method for improving accuracy, such as R. Y. Tsai(1987), J. Weng *et al*.(1992), S. J. Maybank *et al*. (1992), Z. Zhang *et al*. (2000) , Yu xiaoyang(2010), Zhao *et al*.(2015). Considering multi-camera calibration, Svoboda T *et al*. (2005) proposed a fully automatic method and a freely moving bright spot is the only calibration object. Wang (2014) proposed a novel calibration method for the multi-camera measurement system. For large field of view, Liu *et al*. (2015), suggested to use combined small targets for calibration. However, for the infrared camera, its unique imaging way makes it impossible to apply the calibration approach for the visible light cameras directly to the infrared camera. According to the features of the infrared camera, we can modify the calibration approach for the visible light cameras and make it available for the infrared cameras. For instance, Michael Gschwandtner *et al*. (2011) extended the traditional visible light camera calibration methods. They added the resistor array which can generate the infrared radiation on the normal chessboard calibration board to make the board recognized by the infrared camera and consequently, achieved the calibration for the infrared camera. And, Rongqian Yang *et al*. (2011) designed a trinocular vision system to achieve the infrared camera calibration.

ISSN: 1975-0080 IJMUE

The system consisted of two visible light cameras and an infrared camera. The calibration board is made of a black plastic board which is embedded with 25 LEDs. Moreover, Gutschwager, B *et al*. (2015) gives an analysis of the radiometric properties of different types of reference sources applied for the characterization and calibration of infrared cameras.

In this paper, we take the binocular vision system to establish the 3D temperature field and use OpenCV to achieve the calibration work of the two infrared cameras. First of all, we make a calibration board which can be identified by the infrared camera. Then, we use the infrared cameras to take multiple sets of pictures and through programming, finish the calibration for the single infrared camera and the stereo calibration. Furthermore, we apply the SIFT algorithm to obtain the key points of the images and finish the match. After the match, we obtain the 3D information based on triangulation. At last, we carry out an experiment to verify the accuracy of our calibration result.

2. Calibration of the Single Infrared Camera

2.1. Calibration with OpenCV

In this paper, we use OpenCV to calibrate the infrared cameras. The calibration approach that OpenCV uses is an approach between the traditional calibration approach and self-calibration approach, which is proposed by Zhang Zhengyou. The approach is much more flexible than the traditional calibration approach due to the fact that it doesn't need to strictly control the movement of the calibration board.

In OpenCV, we have 4 intrinsic parameters and 5 distortion parameters to solve. To solve the 5 distortion parameters, we can use the 6 pieces of information offered by 3 corner points in one chessboard view. Likewise, we can also use the same chessboard view to solve the intrinsic parameters. For the extrinsic parameters, we need to know 3 rotation parameters (ψ, φ, θ) and 3 translation parameters (Tx,Ty,Tz). Hence, for each chessboard view, we need to calculate 4 intrinsic parameters and 6 extrinsic parameters. Assume that there are N corner points and K chessboard images and to solve the 10 parameters, we need to have $2NK \geq 6K+4$ ($K>1$). In practice, we need at least 10 images with a 7×8 or larger chessboard pattern to increase the calibration accuracy.

After the calibration of the single infrared camera, we also need to implement the stereo calibration for the binocular vision system. If the left and right infrared cameras have been calibrated respectively, then the extrinsic parameters of the two cameras can be denoted as Rl,Tl, Rr and Tr. For an arbitrary point in the space, assume that its world, left-camera and right-camera inhomogeneous coordinates are xw,xl and xr and we can have:

$$x_l = R_l x_w + T_l, x_r = R_r x_w + T_r \tag{1}$$

Consequently, we can have the geometric relation of the two infrared cameras, which are shown as follow:

$$R = R_r R_l^{-1}, T = T_r - R_r R_l^{-1} T_l \tag{2}$$

In the equation, R indicates the rotation matrix and T indicates the translation matrix.

When the calibration board is placed in different positions, we can have different R and T.

At this time, we can take the average value as the optimal calibration result.

According to the theory above, we implement the single and stereo calibration experiments for the infrared cameras based on OpenCV 2.4.3 and Visual Studio 2010.

2.2. Calibration Board for the Infrared Camera

For the visible light cameras, the chessboard pattern is a classical calibration pattern, which can achieve the calibration conveniently. Under the infrared camera, however, the normal chessboard pattern has no obvious difference in heat radiation, which makes its image present little texture information (shown in Figure 1) and make the chessboard pattern disqualified to be the calibration pattern for the infrared cameras. Therefore, in order to calibrate the infrared cameras with OpenCV, we need to make a calibration board that can present a clear image under the infrared camera.

Due to the fact that the chessboard pattern is convenient for the calibration, we imitate the chessboard pattern and make a calibration board that fits the infrared cameras. First of all, we print a normal chessboard pattern and attach it on a black cardboard. Then, hollow out the white squares of the chessboard pattern, together with the cardboard under the squares. Likewise, the left cardboard can be the calibration board of the infrared cameras, which is shown in Figure 2.

Attach the calibration board onto the surface of the heat source, such as the back of the laptop, the monitor and the human body. The hollowed parts and the black parts of the board have different heat radiation, which will present different grayscale under the infrared cameras. The calibration board under the infrared camera is shown in Figure 3.

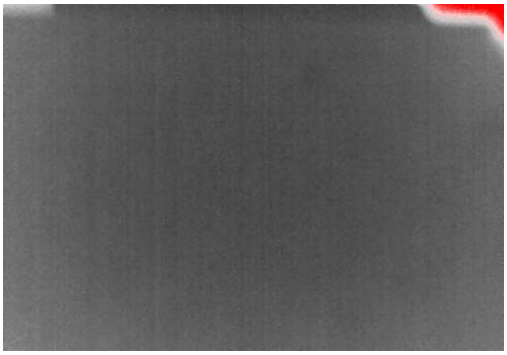

Figure 1. The Normal Chessboard Pattern

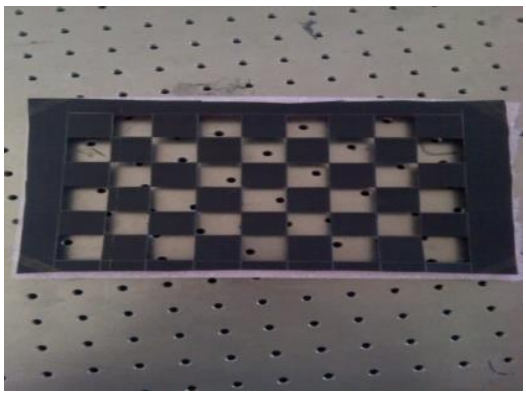

Figure 2. The Calibration Board for the Infrared Camera

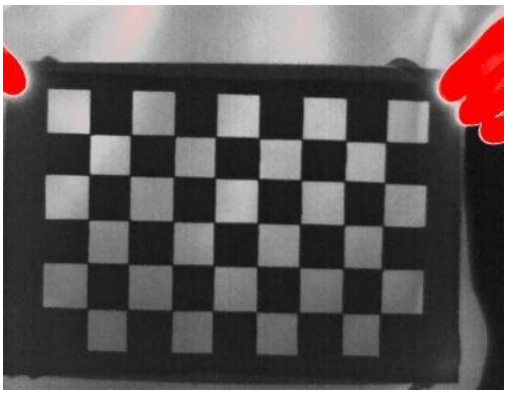

Figure 3. The Calibration Board under the Infrared Camera

2.3. Calibration Experiment

In the binocular vision system, calibrating the two single infrared cameras respectively can guarantee the accuracy of the upcoming stereo calibration and increase the stability of the calibration result. In our experiment, we take ThermoProTM TP8S as our infrared camera, of which the resolution is 384x288 and the pixel size is 25μm.

The single-camera calibration can be described as follows:

1. Take images for the calibration board with different postures (at least 3 images);
2. Detect the corners in each image and save the coordinates of the corners;
3. Process the extracted corners into sub pixels and draw the corners out, which is shown in Figure 4;
4. Calculate the intrinsic and extrinsic parameters of the infrared cameras according to the corners information of each image.

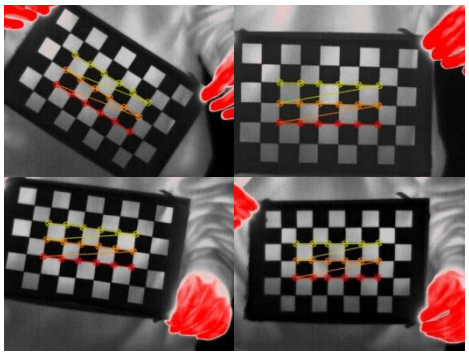

Figure 4. Detect and Draw the Corners

Through calibration, we obtain the parameters of the two infrared cameras, which is displayed in Table 1.

Table 1. Intrinsic Parameters of the Two Infrared Cameras

Parameters	Left Infrared Camera	Right Infrared Camera
F_x	1494.22	1668.58
F_y	1476.59	1637.74
U_0	201.66	197.23
V_0	193.64	193.12
K_1	-1.42	0.15
K_2	642.50	598.78
P_1	0.04	0.04

P_2	0.09	0.14
K_3	-32902.30	-36260.70

After obtaining the intrinsic and extrinsic parameters, we calculate the average re-projecting error to verify the accuracy of the calibrated parameters. Through calculation, the average re-projecting error of the left infrared camera is 0.136 pixels and the average re-projecting error of the right one is 0.138 pixels. The reasons that cause the calibration error are mainly as follows: 1. The made calibration board is not with a high level of precision and consequently causes the inaccuracy of the calibrated parameters; 2. Due to the quality of the images, the number of the detected corners is a little bit less, which cause the convergence of the equations does not reach optimal when calculating the parameters.

3. Stereo Calibration for the Infrared Cameras

3.1. Text Stereo Calibration and Rectification

After calibrating the left and right infrared camera respectively, we can implement the stereo calibration to obtain the positional relation between the two cameras, which is denoted by the rotation matrix R and the translation matrix T.

In OpenCV, function cvStereoCalibrate() is used to implement the stereo calibration and the returning values of the function are the rotation matrix R and the translation matrix T. In our experiment, the obtained rotation matrix is R=[-0.00155601,0.00753352,0.00696552] and the translation matrix is T=[-25.3369,-0.508771,-12.2479].

After the stereo calibration, we need to implement stereo rectification to the images. In our paper, the acquired projecting matrix Q after the stereo rectification is:

$$Q = \begin{bmatrix} 1 & 0 & 0 & 613.589 \\ 0 & 1 & 0 & -147.104 \\ 0 & 0 & 0 & 1636.64 \\ 0 & 0 & -0.03553 & 0 \end{bmatrix}$$

Figure 5 shows the images after the stereo rectification. From the figure, we can see that the left and right images ‘strictly’ align in row after the rectification.

Figure 5. Images after the Rectification

3.2. Matching Experiment for the Infrared Images

The resolution of the infrared camera is low and the texture of the image is not rich. Therefore, by referring to Lowe, D. G (2004) and Bai, Junfeng (2014), we use SIFT algorithm achieve the infrared images match.

Here, we make the images captured by the left infrared camera the training images and the images captured by the right infrared camera the testing images. The matching step for the infrared images are:

1. Detect the SIFT key points in the training images and extract the feature descriptors;
2. Detect the SIFT key points in the testing images and extract the feature descriptors;
3. Match the descriptors of the training and testing images and get the two descriptors of the nearest Euclidean distance among all the descriptors;
4. Get the good matching couples and finish the matching work of the two images.

In our experiment, we have 41 matching couples in total, part of which are shown in Table 2.

Table 2. Coordinates of Some Matching Couples (Pixel)

Matching Couples	Left Image	Right Image
1	[133.295, 4.801]	[101.245, 8.688]
2	[179.975, 123.809]	[143.031, 127.754]
3	[306.768, 168.703]	[269.313, 172.846]
4	[70.964, 30.841]	[39.278, 33.478]
5	[94.629, 32.320]	[62.229, 37.021]
6	[151.604, 77.997]	[115.912, 83.252]
7	[160.474, 79.536]	[125.924, 84.825]
8	[306.768, 168.703]	[270.291, 171.180]
9	[101.157, 37.977]	[68.1996, 42.712]
10	[101.157, 37.977]	[68.1996, 42.712]

The two images have been rectified and therefore, the feature point and its corresponding matching point are in the same row, which are shown in Figure 6.

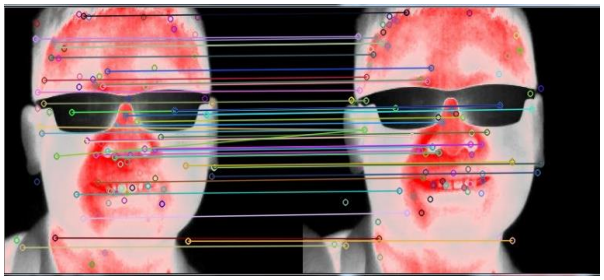

Figure 6. Images after the Rectification

4. Reconstruction Experiment

After the calibration, stereo rectification, matching and disparity calculation, we can obtain the 3D information of the space points.

In this paper, we choose several space points and through comparing the actual measured distance between two certain points with the calculated distance, we verify the accuracy of the calibration result.

We choose five space points which are marked A, B, C, D and E. Through triangulation, we get the spatial coordinate information of the five points, which are shown in Table 3.

Table 3. The Spatial Coordinate of the Chosen Points

	Pixel Coordinate(pixel)	Spatial Coordinate(mm)
A	(176.176,156.934)	(-653.2,-8.1,-1335.4)
B	(165.260, 64.917)	(-658.3, 69.5, -1335.4)
C	(191.593, 110.796)	(-624.6, 28.2, -1335.4)
D	(237.058, 134.767)	(-659.0, 9.6, -1267.9)
E	(140.342, 128.893)	(-578.7, 14.0, -1256.3)

After getting the spatial coordinates of the five points, we compare the calculated distance between two certain points with the actual measured one, of which the results are shown in Table 4.

Table 4. Distance Comparison (Mm)

	Actual Distance	Calculated Distance	Relative Error
AB	79	77.8	1.5%
BC	51	53.3	4.5%
CD	43	39.1	9.1%
DE	77	80.4	4.4%
AC	40	46.2	15.5%
BD	70	59.9	14.4%
BE	70	62.4	10.9%
CE	51	48.0	5.9%

From the experimental results, we can see that the calculated distance is close to the actual measured distance, which proves the calibration result is relatively accurate. However, the accumulated error cause the inaccuracy in calculation. We can improve the precision of the calibration board and operate more carefully in each calibrating step to obtain a more accurate calibration result.

5. Conclusions

The 3D temperature field reconstruction can obtain the depth information which is lost in 2D temperature image and can consequently be applied in the detection and maintenance of the complex objects. It can be widely used in various fields.

Based on the binocular vision system and with the help of OpenCV, we achieve the calibration of the infrared cameras, which is a crucial step in the reconstruction of the 3D temperature field. First of all, we make a calibration pattern that can be clearly captured by the infrared camera and finish the single infrared camera calibration. Then, we implement the stereo calibration and rectification for the infrared cameras. Finally, we calculate the 3D coordinates of a certain point in space through key points matching and triangulation.

According to the experimental results, the calibration results of the infrared cameras are basically accurate, of which the re-projecting error is small. Moreover, the calculated distance is close to the actual measured one, but the error still exists and the average value is 8.3%.

Acknowledgement

This study was supported by Scientific and Technological Project of Education Department of Heilongjiang Province with grant number (12541171).

References

[1] D. Gennery, "Stereo-camera calibration", In Proceedings of the 10th Image Understanding Workshop, **(1979)**, pp. 101-108.
[2] R. Y. Tsai, "A versatile camera calibration technique for high-accuracy 3D machine vision metrology using off-the-shelf TV cameras and lenses", IEEE Journal of Robotics and Automation, vol. 3, no. 4, **(1987)**, pp. 323-344.
[3] J. Weng, P. Cohen and M. Herniou, "Camera calibration with distortion models and accuracy evaluation", IEEE Transactions on Pattern Analysis and Machine Intelligence, vol. 14, no. 10, **(1992)**, pp. 965-980.
[4] S. J. Maybank and O. D. Faugeras, "A theory of self-calibration of a moving camera", International Journal of Computer Vision, vol. 8, no. 2, **(1992)**, pp. 123-152.
[5] Z. Zhang, "A flexible new technique for camera calibration", IEEE Transaction Pattern Analysis and Machine Intelligence, vol. 22, no. 11, **(2000)**, pp. 1330 -1334.
[6] Y. Xiaoyang, S. lina, C. shennan and W. Haibin, "The review of structured light time encoding technologies", Journal of Harbin University of Science and Technology, vol. 15, no. 1, **(2010)**, pp. 98-102.
[7] Z. Huijie, W. Zhen and J. Hongzhi, "Calibration for stereo vision system based on phase matching and bundle adjustment algorithm", Optics and Lasers in Engineering, vol. 68, **(2015)**, pp. 203-213.
[8] T. Svoboda, D. Martinec and T. Pajdla, "A Convenient Multi-camera Self-calibration for Virtual Environments", PRESENCE: Tele operators and Virtual Environment, vol. 14, no. 4, **(2005)**, pp. 407-422.
[9] W. Xinlei, "Novel Calibration Method for the Multi-Camera Measurement System", Journal of the Optical Society of Korea, vol. 18, no. 6, **(2014)**, pp. 746-752.
[10] L. Zhen, L. Fengjiao and L. Xiaojing, "A novel and accurate calibration method for cameras with large field of view using combined small targets", Measurement, vol. 64, **(2015)**, pp. 1-16.
[11] M. Gschwandtner, "Infrared Camera Calibration for Dense Depth Map Construction", 2011 IEEE Intelligent Vehicles Symposium (IV)Baden-Baden, Germany, vol. 5-9, **(2011)**, pp. 857-862.
[12] R. Yang, "Geometric Calibration of IR Camera Using Trinocular Vision", Journal of Lighwave Technology, vol. 29, **(2011)**, pp. 3793-3803.
[13] B. Gutschwager, D. Taubert and J. Hollandt, "Analysis of Reference Sources for the Characterization and Calibration of Infrared Cameras", International journal of thermophysics, vol. 36, no. 2-3, **(2015)**, pp. 303-314.
[14] D. G. Lowe, "Distinctive Image Features from Scale-Invariant Keypoints", International Journal of Computer Vision, vol. 60, no. 2, **(2004)**, pp. 91-110.
[15] B. Junfeng, M. Yong and L. Jing, "Good match exploration for thermal infrared face recognition based on YWF-SIFT with multi-scale fusion", Infrared physics & technology, vol. 67, **(2014)**, pp. 91-97.

